Heat transfer in flat-plate boundary layers: a correlation for laminar, transitional, and turbulent flow

Heat Transfer in Flat-Plate Boundary Layers: A Correlation for Laminar, Transitional, and Turbulent Flow

John H. Lienhard V
Fellow ASME
Abdul Latif Jameel Professor
Rohsenow Kendall Heat Transfer Laboratory,
Department of Mechanical Engineering,
Massachusetts Institute of Technology,
Cambridge, MA 02139-4307
e-mail: lienhard@mit.edu

The laminar and turbulent regimes of a boundary layer on a flat plate are often represented with separate correlations under the assumption of a distinct "transition Reynolds number." Average heat coefficients are then calculated by integrating across the "transition point." Experimental data do not show an abrupt transition, but rather an extended transition region in which turbulence develops. The transition region may be as long as the laminar region. Although this transitional behavior has been known for many decades, few correlations have incorporated it. One attempt was made by Stuart Churchill in 1976. Churchill, however, based his curve fit on some doubtful assumptions about the data sets. In this paper, we develop different approximations through a detailed consideration of multiple data sets for $0.7 \leqslant Pr \leqslant 257$, $4000 \leqslant Re_x \leqslant 4,300,000$, and varying levels of freestream turbulence for smooth, sharp-edged plates at zero pressure gradient. The result we obtain is in good agreement with the available measurements and applies smoothly over the full range of Reynolds number for either a uniform wall temperature or a uniform heat flux boundary condition. Fully turbulent air data are correlated to $\pm 11\%$. Like Churchill's result, this correlation should be matched to the estimated transition condition of any particular flow. We also review the laminar analytical solutions for a uniform wall heat flux, and point out limitations of the classical Colburn analogy. [DOI: 10.1115/1.4046795]

Keywords: turbulent boundary layer, turbulent transition, laminar boundary layer, heat transfer coefficient, Nusselt number, plate, correlation, similarity solution, unheated starting length

1 Introduction

Simplified treatments of boundary layer heat transfer split the boundary layer into an upstream laminar section and downstream turbulent section. Correlations are then formed for these two sections, which are assumed to be separated by a distinct transition Reynolds number. An example is the correlation for average heat transfer coefficient proposed by Whitaker [1]: the heat transfer coefficient is averaged over the length, using results from laminar theory and correlation for turbulent flow. A transition Reynolds number of 200,000 is assigned, and single equation depending on the overall Reynolds number is obtained.

The actual transition process has long been known to include a lengthy transition region, in which the heat transfer coefficient rises smoothly. Indeed, data show this region to have a length similar to the laminar region (see Sec. 4).

In contrast to Whitaker, Churchill [2] proposed a continuous correlation to predict the local Nusselt number, Nu_x, from laminar flow, through the transition region, and into the turbulent region. He used an algebraic combining formula to smoothly join a laminar correlation, $\mathrm{Nu}_{\mathrm{lam}}$, a transitional correlation, $\mathrm{Nu}_{\mathrm{trans}}$, and a turbulent correlation, $\mathrm{Nu}_{\mathrm{turb}}$. He also included an additive constant, Nu_0, for very low Reynolds numbers

$$\mathrm{Nu}_x = \mathrm{Nu}_0 + \left[\mathrm{Nu}_{\mathrm{lam}}^s + \left(\mathrm{Nu}_{\mathrm{trans}}^p + \mathrm{Nu}_{\mathrm{turb}}^p\right)^{s/p}\right]^{1/s} \tag{1}$$

In Eq. (1), all four terms are included irrespective of the value of Re_x. Each term will become dominant in the appropriate range, as ensured by the exponents used and the terms' differing dependence on Re_x [3]. Churchill's values of $p = -5$ and $s = 2$ produce fairly gradual transitions between the three indicated ranges. To account for the variability of transition, his result must be matched to any particular dataset by fitting the value of Reynolds number at the upper limit of the transition region, Re_u, into his formula for $\mathrm{Nu}_{\mathrm{trans}}$.

Churchill expressed the three variable terms as functions of a single parameter, $\phi(\mathrm{Re}_x, \mathrm{Pr}) = \mathrm{Re}_x \mathrm{Pr}^{2/3}\left[1 + (d/\mathrm{Pr})^{2/3}\right]^{-1/2}$, with different values of d for uniform wall temperature (UWT) or for uniform heat flux (UHF)

This function was based upon his and Ozoe's laminar flow curve-fits spanning all values of Pr [2,4]. As a consequence, he had to make an approximation for the turbulent Nusselt number. The full statement of Churchill's equation is given in Appendix A.

Churchill compared his model to aggregated data for the local and average heat transfer coefficient, with partial agreement. As seen in Fig. 1, the overall agreement with local data is not close. The transition away from laminar flow begins too soon, the slope in the transition region does not match, and the values in the fully turbulent range are slightly high. Therefore, a more accurate fit is desirable.

Here, we develop a correlation that accurately captures the lengthy transition region. The available data sets are reviewed together with key theoretical points so that differences among the measurements will be more clear. Churchill's basic concept is retained, but its primary elements are reëvaluated. The resultant equation is compared to a large number of independent measurements. The measurements clearly indicate that the transition Nusselt number rises more rapidly with Reynolds number when transition begins at a higher Reynolds number. We offer a straightforward formula for calculating the local (and average) heat transfer coefficient, which has good agreement with data in the literature.

In any situation for which both the laminar and turbulent regimes must be considered, so should be the transitional region.

Contributed by the Heat Transfer Division of ASME for publication in the Journal of Heat Transfer. Manuscript received December 1, 2019; final manuscript received March 2, 2020; published online April 27, 2020. Assoc. Editor: Ranga Narayanan.

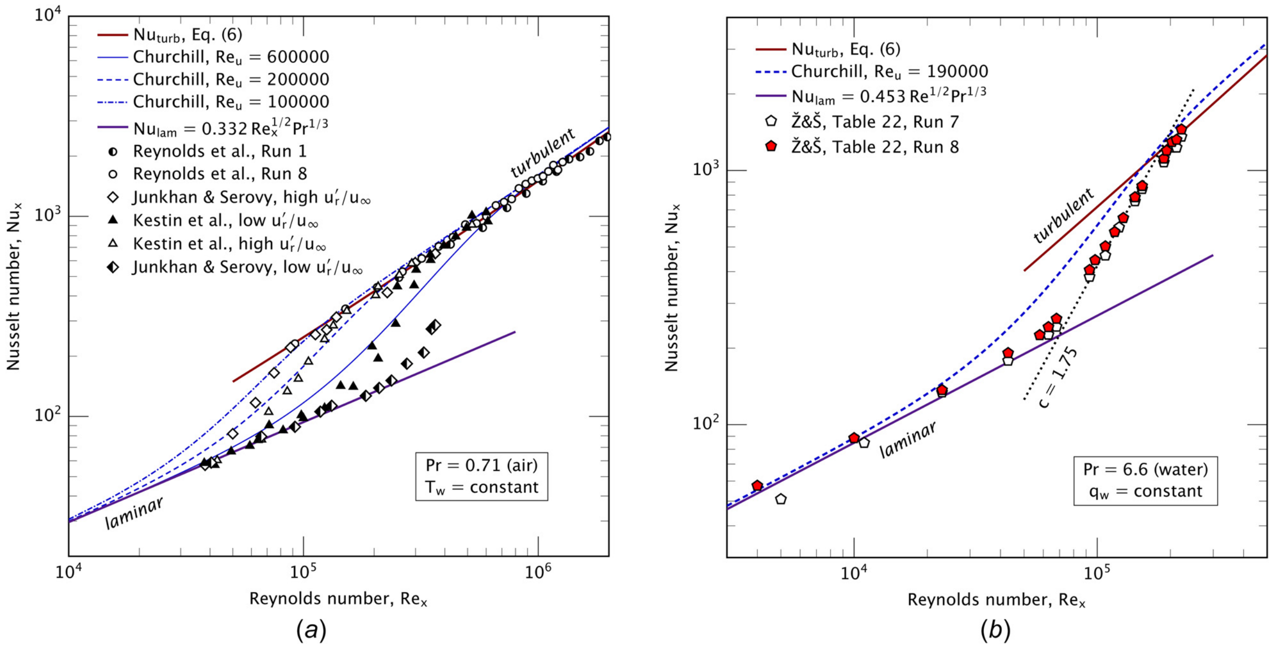

Fig. 1 Churchill's correlation, Eq. (A1), applied to air and water experiments. u_r' is the root-mean-square turbulent fluctuation relative to the mean freestream speed, u_∞. (a) air data from several investigators [10,17,32], and (b) water data from Žukauskas and Šlančiauskas [26].

This fact is particularly important if local values of the heat transfer coefficient are required.

2 Theoretical Considerations and Assessment of Available Data Sets

The theory of boundary layer heat transfer is today very highly developed. To understand the differences in the data sets, a few fundamental points need to be in mind. These ideas are highlighted briefly, with no intention to give a comprehensive account.

2.1 Laminar Boundary Layers. Most differences between the laminar measurements used herein and the laminar theory can be attributed to differences in the wall boundary condition and/or in the upstream initial conditions.

The heat transfer coefficient in a laminar boundary layer is strongly sensitive to the upstream history of the flow, including both the leading-edge configuration and any variation in wall temperature. Most of the experimental reports have taken care to describe leading-edge conditions. In some studies, upstream boundary layers were suctioned away through a slot ahead of the test piece. Most of the experiments had an unheated initial length or an initial section in which temperatures were not well controlled, and most of those experimentalists applied analytical correction factors to make their reported data appear as if the initial length were uniform (Blair [5] is notable for giving a clear account of the unheated region and reporting it without adjustment; see Sec. 4.).

The local heat transfer coefficient in a flat-plate boundary layer is higher for UHF than for UWT, by the factor of $0.453/0.332 = 1.36$ [6]. While that knowledge, as an experimental result with partial theoretical support, was available in the 1930s [7], many noteworthy heat transfer researchers were unaware of this fact during the 1940s and 1950s (see Appendix B). Instead, these researchers benchmarked laminar data on Pohlhausen's UWT solution [8].[1] For example, Jakob and Dow [9] questioned the work of Fage and Falkner [7] on electrically heated platinum strips for being 27% above Pohlhausen's result; further, they reported that A.P. Colburn came to a similar opinion after they wrote to him. Likewise, Kestin et al. [10] were very critical of the transient measurements of Sugawara et al. [11] for this same reason. Yet, Sugawara's laminar measurements (and correlation) agree well with the analytical formula for a uniform wall heat flux; and the 1951 Japanese-language version of their work [12] explicitly considers a wall temperature varying as $x^{1/2}$ (as it would for a uniform heat flux), contrasting that result to Pohlhausen's formula.[2]

2.2 Freestream Turbulence. Freestream turbulence is normally manipulated by placing a grid of bars upstream of the test plate; the formation and decay of grid turbulence have been very well understood in the wind-tunnel literature since the late 1930s [13,14].

Experimentalists concluded early on that freestream turbulence at levels up to 5% or so had little or no effect on the laminar heat transfer coefficient [7,15]. Experiments also clearly showed that increasing freestream turbulence strongly reduced the transition Reynolds number and that, with extremely low turbulence, the onset of transition could be delayed to $Re_x \simeq 2.8 \times 10^6$ [16]. However, the effect of freestream turbulence on heat transfer in the turbulent boundary layer was extensively debated during the mid-twentieth century [7,10,11,15,17]. Mainly, these early investigations concluded that freestream turbulence had little effect at zero pressure gradient (the work of Sugawara et al. [11] is an exception). Eventually, more precise measurements encompassing higher turbulence levels showed that freestream turbulence can modestly increase the turbulent heat transfer coefficient. Blair [5], for example, measured up to an 18% increase for a nominal freestream turbulence level of 6%.

In what follows, we consider data with reported freestream turbulence levels below 5% (and mostly below 3%).

The various experimental reports differ significantly on how turbulence was characterized. Blair, for example, used multicomponent hot-wire anemometer measurements to fully describe the

[1]In modern notation, Pohlhausen's equation is $Nu_x = 0.332\,Re_x^{1/2}Pr^{1/3}$.

[2]Sugawara et al. measured the transient heating and cooling of a plate in a wind tunnel at a dozen positions along the plate. The plate temperature response, locally, was treated as lumped. The plate would cool faster near the leading edge.

streamwise variation of the turbulence in each case. In other cases, experimentalists have reported only, say, "about 0.3%" without elaboration [18]. The length and time scales of turbulence in the various experimental systems differ and cannot productively be compared using only the reported value of u'_r/u_∞. However, variation of turbulence within a single experimental system is clearly comparable within that system. We note the level of freestream turbulence of the data sets whenever it has been reported.

2.3 Turbulent Boundary Layers. Heat transfer coefficients in turbulent boundary layers are not sensitive to slow streamwise variations in the wall temperature, and the value of h for UHF is only about 4% greater than for UWT [19].

The near-wall velocity distribution in the fully turbulent boundary layer is essentially a function of the local wall shear stress, as embodied by the universal velocity profile or "law-of-the-wall" [20,21]. Similarly, the local heat transfer coefficient for nonmetallic fluids is mainly determined by the *local* shear stress and the Prandtl number, as shown by the Reynolds–Colburn analogy [22,23] and its more accurate generalizations based on boundary-layer structure [6,24,25]. For the internal flow case, shear stress is represented by the Darcy friction factor, proportional to $f/8$, while the external flow case uses the skin friction coefficient, as $C_f/2$.

Data for external, turbulent boundary-layer heat transfer have mainly been acquired in air flows. Water boundary layers have been measured, apparently, only by Žukauskas and Šlančiauskas [26] and by Hollingsworth [27]. Data for other liquids are even more limited, amounting to measurements in "transformer oil," again by Žukauskas and coworkers. This situation could seem discouraging until one recalls that a vast body of data exists for turbulent internal flow (in pipes), spanning an enormous range of Prandtl number. As a consequence of the universal velocity distribution, the generalized Reynolds–Colburn analogy for pipe flows is directly adaptable to the external boundary layers on a flat plate in nonmetallic, low-speed flows. Thus, the exhaustive correlations for internal flow in terms of $f/8$ can support the calculation of h from $C_f/2$ for those Pr at which external flow measurements have not been made (i.e., for most fluids other than air). We shall reinforce this point in this paper by comparison to data for air, water, and transformer oil.

The relevant generalization of the Reynolds–Colburn analogy is

$$\mathrm{St} = \frac{\mathrm{Nu}_x}{\mathrm{Re}_x \mathrm{Pr}} = \frac{C_f/2}{a_1 + a_2(\mathrm{Pr}^{a_3} - 1)\sqrt{C_f/2}} \tag{2}$$

Various authors have proposed values for the coefficients $\{a_1; a_2; a_3\}$. For example, Prandtl [28] chose $\{1; 8.77; 1\}$ (pipe flow); Žukauskas and Šlančiauskas [26] proposed $\{0.93; 12.5; 2/3\}$ (flat plate); White [25] gave $\{1; 12.8; 0.68\}$ (flat plate); and Petukhov [29] gave $\{1.07; 12.7; 2/3\}$ (pipe flow). Gnielinski [30] examined thousands of data points in pipe flow, spanning $0.6 \leqslant \mathrm{Pr} \leqslant 10^5$, leading him to suggest $\{1; 12.7; 2/3\}$. Gnielinski's values capture 90% of the liquid data to $\pm 20\%$, with even better agreement for gases. In what follows, we adopt Gnielinski's coefficients.

Theoretical considerations have suggested the use of virtual origins or of the enthalpy thickness in correlating boundary layer data [19,27,31], but here we focus on the local Reynolds number because that is how the vast majority of the data have been presented.

2.4 Variable Property Effects. For boundary layers with large temperature differences, property variation across the boundary may be important. For turbulent gas flows, property corrections are often made by evaluating a correlation at T_∞ and multiplying the result by the absolute temperature ratio, $(T_w/T_\infty)^{-n}$, with n between 0.25 and 0.4 [26,32]. (For pipe flow, Gnielinski recommends $n = 0.45$ [30]). For the air data discussed here, temperature ratios are less than 1.11, and property variations are either negligible or small ($\lesssim 5\%$). No corrections are applied in plotting the correlations for air data in what follows.

For liquids, corrections are generally based on a ratio of viscosities or Prandtl numbers, and most data are for turbulent pipe flows. For external boundary layers, the most comprehensive experimental study is due to Žukauskas and Šlančiauskas [26], who recommend evaluating Nusselt number correlations using properties at T_∞ and multiplying the result by $(\mathrm{Pr}_\infty/\mathrm{Pr}_w)^{0.25}$. (For turbulent pipe flow, Gnielinski recommends an exponent of 0.11). Typical values of the Prandtl number for the fluids discussed here are given in Appendix D.

For the water data used herein, the property corrections are modest, ranging from <2% to 6%, with a single run (discussed below) reaching 10%. No corrections have applied to the water correlations in the plots shown.

For transformer oil, however, the corrections can exceed 20%; these will be addressed in context.

2.5 Data Sets Examined. For this study, measurements of the local heat transfer coefficient through transition region are of primary interest. The data sets for local heat transfer coefficients are described in Tables 1 and 2. These data are used in examining the variation of the heat transfer coefficient in the transition region.

Data sets for average heat transfer coefficients are summarized in Table 3 because they were used by Churchill [2], Whitaker [1], and others in developing correlations. Apart from the laminar study of Fage and Falkner [7], those data sets are strongly affected by unheated starting lengths and other geometric differences, so we will not consider them in any detail.

3 Reconstituting Churchill's Formula

The term Nu_0 in Eq. (1) is intended to account for heat transfer at very low Reynolds numbers, as for creeping flow. Churchill selected $\mathrm{Nu}_0 = 0.45$ on the basis of numerical simulations for $\mathrm{Pr} = 1$ by Dennis and Smith [40] and without experimental support. The contribution of Nu_0 is negligible for Reynolds numbers greater than 1000 or so in nonmetallic liquids. We shall restrict our attention to nonmetallic liquids, with $\mathrm{Pr} \geqslant 0.6$ and $\mathrm{Re}_x \gtrsim 1000$, and omit Nu_0.

For the laminar boundary layer, Churchill used his and Ozoe's fits over all Pr [2,4], introducing the function $\phi(\mathrm{Re}_x, \mathrm{Pr})$ mentioned in Sec. 1. Having limited the range to $\mathrm{Pr} \geqslant 0.6$, we only need the common results for laminar boundary layers on sharp-edged flat plates

$$\mathrm{Nu}_{\mathrm{lam}} = a\,\mathrm{Re}_x^{1/2}\,\mathrm{Pr}^{1/3} \quad \text{for } \mathrm{Pr} \geqslant 0.6 \tag{3}$$

where $a = 0.332$ for UWT or 0.453 for UHF [6].

In the transition region, Churchill proposed a curve fit

$$\mathrm{Nu}_{\mathrm{trans}} = b\,\mathrm{Re}_x^c \tag{4}$$

The value of b is fixed by either the value of $\mathrm{Nu}_{\mathrm{lam}}$ at the Reynolds number where transition starts, Re_l, or the value of $\mathrm{Nu}_{\mathrm{turb}}$ at the upper end where transition ends, Re_u. Churchill selected the latter; we shall use the former because the laminar equations are better defined. Thus

$$\mathrm{Nu}_{\mathrm{trans}} = \mathrm{Nu}_{\mathrm{lam}}(\mathrm{Re}_l, \mathrm{Pr})\,(\mathrm{Re}_x/\mathrm{Re}_l)^c \tag{5}$$

Churchill suggested a fixed exponent of $c = 3/2$, which seemed to fit some of Žukauskas and Šlančiauskas' data sets [26]; the latter authors had suggested 1.4. In contrast, our comparison to data in Sec. 4 shows c is usually larger than this and that the value c rises as Re_l rises. Our approach will be to treat c as a function of Re_l in fitting the data.

Table 1 Data sets for local heat transfer coefficients in air. All are wind tunnel measurements. Boundary condition (B.C.), r.m.s. freestream turbulence (u_r'/u_∞), and temperature difference across boundary layer (ΔT) are as indicated.

Authors and years	B.C.	Range of Re_x	u_r'/u_∞	ΔT (K)	Comments
Blair, 1982/3 [5,33,34]	UHF	$1.1 \times 10^4 - 4.5 \times 10^6$	0.2–9.0%	<20	Upstream grid produced freestream turbulence, with thorough documentation. "Nominal" u_r'/u_∞ from 0.25 to 6%, decaying along plate length. Includes 4.3 cm unheated starting length, without data corrections and in excellent agreement with laminar theory. Uncertainties (2σ?): St $\pm$ 2.5%; Re_x $\pm$ 1%.
Junkhan and coworkers, 1964/7 [17,35]	UWT	$3.8 \times 10^4 - 3.6 \times 10^5$	0.4–1.8%	~17	Upstream grid produced freestream turbulence: no grid, 0.4–0.8%; with grid, 1.3–1.8%. Data corrected for the unheated starting length. Temperature controlled by rows of electrically heated strips. Uncertainties (2σ): Nu_x $\pm$ 5.2%; Re_x $\pm$ 2.5%.
Kestin et al., 1961 [10]	UWT	$3.5 \times 10^4 - 6.0 \times 10^5$	0.7–3.8%	35–44	Upstream screen produced freestream turbulence. Low turbulence set has u_r'/u_∞ of 0.75–1.6%; high turbulence set has 3.1–3.8% in front section and 2.4–3.0% in back section. Plate temperature was steam controlled; data corrected (~5%) for leading-edge temperature variation. Uncertainties described in Ref. [10].
Reynolds et al., 1958 [32,36]	UWT	$9.2 \times 10^4 - 3.5 \times 10^6$	2.0–4.8%	10–14	Fully turbulent flow, b.l. tripped at the leading edge. u_r'/u_∞ typically 2–3% over most of plate, but exceeded 4.5% for highest speeds. Temperature controlled by rows of electrically heated strips. Uncertainties (1σ): St $\pm$ 3%; Re_x $\pm$ 1%. Includes one data set for "natural transition" (low speed, $u_r'/u_\infty = 2$–2.5%).
Seban and Doughty, 1956 [18]	UHF	$1.1 \times 10^5 - 4 \times 10^6$	~0.3%	<14	Wind tunnel with low freestream turbulence. Data were corrected for an unheated nose piece ahead of the thicker test section. The authors state that these corrections contributed some scatter to the transition region data. Uncertainties not clearly stated, although the experiments were carefully designed. Measurement of u_r'/u_∞ not described.
Sugawara et al., 1951/8 [11,12]	$\sim\sqrt{x}$	$4.1 \times 10^3 - 3 \times 10^5$	0.7–7.4%	?	Grids at two distances upstream. Heat transfer coefficients increased 55% at u_r'/u_∞ of 7%. Transient cooling of plate; nonuniform T_w distribution coincidentally like that for UHF, but minimal detail reported. Blunt leading edge caused transition at Re_x of 10,000–20,000 in NACA version [11]. Uncertainties not described.
Žukauskas and Šlanciauskas (1987 summary of older work) [26]	UHF	$1.1 \times 10^4 - 3.2 \times 10^6$	~0.3%	<34	Data of Fig. 4(c) are from experiments around transition region, three runs with varying ΔT. Figure 4(d) shows separate experiments focused on higher Re_x, with significant scatter in laminar flow and Nu_x for turbulent flow about 15% higher than most reports. Book summarizes older works. Uncertainty in heat transfer stated as $\pm$5%.

Table 2 Data sets for local heat transfer coefficients in liquids. Boundary condition (B.C.) and r.m.s. freestream turbulence (u_r'/u_∞) are as indicated.

Authors and years	B.C.	Range of Re_x	u_r'/u_∞	Comments
Data for water				
Hollingsworth and coworkers, 1989 [27,31,37]	UWT	$\approx 5 \times 10^5\%$	0.5–1.5%	Data for $\mathrm{Pr} = 5.93 \pm 0.13$ with 4 K b.l. temperature difference. Boundary layer tripped ahead of plate, with a substantial unheated section; two locations measured in uncurved channel. Plate temperature controlled by rows of electrically heated strips. Data analysis focuses on enthalpy thickness Reynolds number. Data were used to calibrate a numerical model, leading to a correlation: $\mathrm{St} = 0.02426\,\mathrm{Re}_x^{-n}\mathrm{Pr}^{-0.895}$ for $n = 0.1879\,\mathrm{Pr}^{-0.18}$ for $0.7 \leqslant \mathrm{Pr} \leqslant 8$. Measurement uncertainties (2σ): St $\pm$ 3.3%; $\mathrm{Re}_x \pm 1.6\%$.
Žukauskas and Šlančiauskas (1987 summary of older work) [26]	UHF	$4.0 \times 10^3 - 4.4 \times 10^6$	$\sim$1.2%	Data for Prandtl numbers of 2.95, 5.4, and 6.6. Stated uncertainty in heat transfer is up to $\pm$ 10%, being largest for higher fluxes. Background turbulence measured at inlet to test section. For Pr = 5.4: Run 17, ΔT is 7–8 K for the turbulent and transitional data, with the laminar points rising to 17 K; Run 18, $6.5 \leqslant \Delta T \leqslant 21.4$ K; Table 25, ΔT is 7–8 K for the turbulent and transitional data, again rising to 15–17 K in the laminar region. For Pr = 6.6: Run 7, $1.3 \leqslant \Delta T \leqslant 4.2$ K; Run 8, $6.5 \leqslant \Delta T \leqslant 21.4$ K. For Pr = 2.95: $5.4 \leqslant \Delta T \leqslant 8.6$ K.
Data for higher Pr				
Žukauskas and Šlančiauskas (1987 summary of older work) [26]	UHF	$1.2 \times 10^4 - 7.7 \times 10^5$	$\sim$0.7%	Data for "transformer oil" at several Prandtl numbers (55–257). Uncertainty in heat transfer stated as $\pm$ 5%. Background turbulence measured at inlet to test section. Much of this data has significant property variation across the boundary layer (An additional data set is given for cooling hot glycerin at higher Pr, but with even stronger property variations.).

Table 3 Data sets for average heat transfer coefficients with r.m.s. freestream turbulence (u_r'/u_∞) indicated when known

Authors and years	Range of Re_L	u_r'/u_∞	Comments
Fage and Falkner, 1931 [7]	$1.4 \times 10^3 - 1.2 \times 10^4$		Laminar flow over electrically heated platinum strips with varied levels of turbulence. Average strip temperatures were measured from strip electrical resistance. The strips were placed into the centerline of long and short tubes, with or without a screen or perforated plate at the inlet; levels of turbulence were not reported. Freestream turbulence found not to affect laminar heat transfer rate. Temperature ratios were large ($T_{w,\mathrm{av}}/T_\infty = 1.45$). Air thermal conductivity used was 12% less than current value.
Jakob and Dow, 1946 [9]	$4.5 \times 10^4 - 1.5 \times 10^6$		Electrically heated copper section of a cylindrical tube was studied. Tube was placed axially in an open-air jet. Average surface temperature in the copper jacket recorded. Corrections were applied for unheated starting length of varied dimension. Average Nusselt number as a function of overall Reynolds number is reported. Transition to turbulence changed significantly with changes of shape of the unheated nose-piece. Freestream turbulence is not described.
Parmelee and Hueberscher, 1947 [38]	$1.9 \times 10^4 - 9.3 \times 10^5$		Aluminum plate with four heated sections at center which were independently controlled. An "average plate temperature," air speed, and h were tabulated. Leading edge radius was observed to significantly affect h. No uncertainty analysis or freestream turbulence data. Transition is stated to occur at a Reynolds number of 150,000. Data were corrected for natural convection and guard heaters.
Edwards and Furber, 1956 [15]	$5 \times 10^4 - 2.5 \times 10^6$	$\leqslant$5%	Studied freestream turbulence effects on heat transfer in air. A 6 in. electrically heated, copper section was located 33 in. downstream of plate's leading edge. The average temperature of the copper section was taken. Turbulence produced by an upstream grid; background turbulence not reported. Large corrections for the unheated starting length were applied (21–75%). Turbulence found to have only limited effect on heat transfer, but a very strong effect on the location of transition.
Žukauskas and Ambrazyavichyus, 1961 [39]	$2 \times 10^4 - 3 \times 10^7$		Plates up to 250 mm long were either electrically heated or water cooled. The same channel was used for air, water, and transformer oil. Average plate temperatures were found from thermocouples by integration. Heated portion of plate ranged from 11% to 80%; a simple power-law was used to correct the data for the unheated initial length. The average heat transfer coefficient over the heated length, L_0, is reported to be independent of the unheated length and correlated as: $\overline{\mathrm{Nu}}_{L_0} = 0.037\,\mathrm{Re}_{L_0}^{0.8}\,\mathrm{Pr}_\infty^{0.43}(\mathrm{Pr}_\infty/\mathrm{Pr}_w)^{0.25}$ in fully turbulent flow for $0.7 < \mathrm{Pr} < 380$. The scatter of the data about the curve fit is $\pm$15% at a Reynolds number of 1,000,000 and greater for lower Re. Freestream turbulence is not reported.

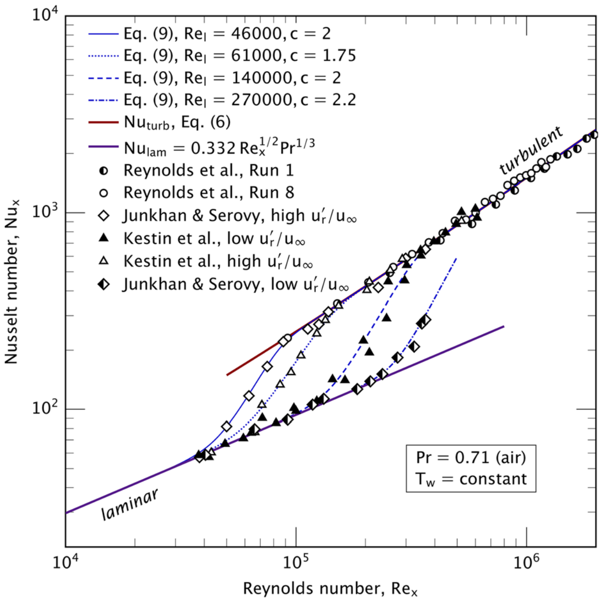

Fig. 2 The proposed correlation, $Nu_x(Re_x, Pr)$ from Eq. (9), compared to constant wall temperature data for air from several investigators [10,17,32]

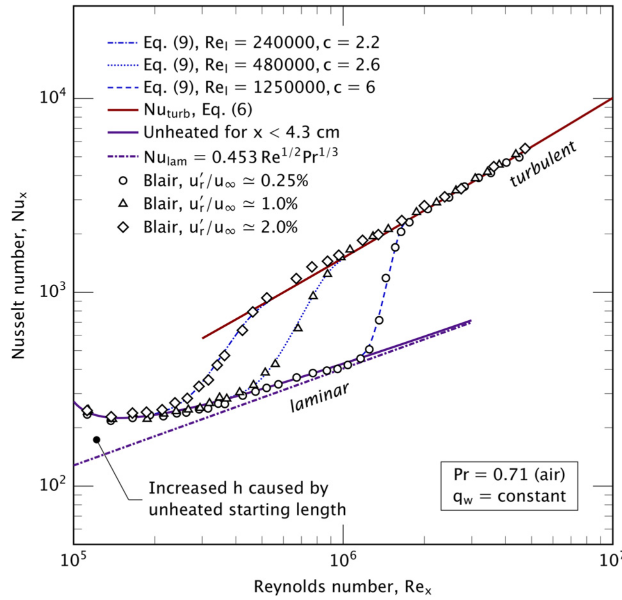

Fig. 3 Proposed correlation, Eq. (9), compared to constant heat flux data of Blair for three levels of freestream turbulence in air [5]. Plate was unheated for $x < x_0 = 4.3$ cm. The analytical result for a laminar, unheated starting length is used for the laminar term in Eq. (9): $Nu_{lam} \times [1-(x_0/x)^{3/4}]^{-1/3}$.

In the turbulent region, Churchill improved a bit, so as to adapt a power-law fit for Nu_{turb} to his ϕ variable (see Appendix A). The resulting equation overpredicts most air data, other than Žukauskas and Šlančiauskas [26]; and the resulting Prandtl number dependence has no experimental support. Instead of working with ϕ, we can directly employ the general form of the Reynolds–Colburn analogy for smooth walls, Eq. (2), as $Nu_{turb} = \mathrm{fn}(Re_x, Pr)$, for either UWT or UHF (see Sec. 2.3)

$$Nu_{turb} = \frac{Re_x Pr\,(C_f/2)}{1 + 12.7(Pr^{2/3} - 1)\sqrt{C_f/2}} \quad \text{for } Pr \geqslant 0.6 \tag{6}$$

The skin friction coefficient, C_f, may be evaluated using White's formula [25,41] to an accuracy of 1–2%

$$C_f(x) = \frac{0.455}{[\ln(0.06\,Re_x)]^2} \tag{7}$$

White recommends this equation for zero-pressure-gradient turbulent boundary layers at any Re_x.

Equation (6) with (7) provides very good agreement with most data over a wide range of Prandtl numbers (see Sec. 4). For gases, the result is well approximated by the power-law proposed by Reynolds et al. [32][3]

$$Nu_{turb} = 0.0296\,Re_x^{0.8}\,Pr^{0.6} \quad \text{for gases} \tag{8}$$

To address the slow transition between regimes in Churchill's fit, different exponents can be applied. We have tested several values. The rather large numbers $p = -10$ and $s = 5$ provide sharper transitions than Churchill's values, better tracking the datasets examined. On this basis, Eq. (1) simplifies

$$Nu_x(Re_x, Pr) = \left[Nu_{lam}^5 + \left(Nu_{trans}^{-10} + Nu_{turb}^{-10}\right)^{-1/2}\right]^{1/5} \tag{9}$$

[3]Reynolds et al. suggest multiplying by variable-properties correction factor of $(T_w/T_\infty)^{-0.4}$, which amounted to about 2% for their data. Their equation fits their data to a standard deviation of ±4.5%.

The three component terms should be calculated from Eqs. (3) and (5), and either Eqs. (6) or (8), rather than Churchill's constructions. The value of Re_l should be fit to the dataset, and the value of c may either be fitted or estimated from Eq. (11), which is discussed in Sec. 4.4. When data are not available, Eq. (12) can provide a very rough estimate of Re_l.

Equation (9) can conveniently be used in a spreadsheet or other software… or by hand if one is old school.

4 Results

Equation (9) is compared to: data for air in Figs. 2–4; data for water in Figs. 6 and 7; and data for oil in Figs. 8 and 9. The transition region has been fitted with the values of c and Re_l shown in the figures. The agreement in the transition region is generally excellent.

4.1 Data for Air.

Figure 2 shows wind tunnel data including the transition region for UWT from Kestin et al. [10] and from Junkhan and Serovy [17]. Values of c and Re_l have been fitted to each of these four data sets, and the corresponding curve from Eq. (9) (with Eqs. (3), (5), (6), and (7)) is plotted. The value of c trends higher as Re_l rises. Also shown, for reference, are two sets of fully turbulent measurements from Reynolds et al. [32]; the latter are in excellent agreement with both Eqs. (6) and (8). Reynolds et al. reported six additional data sets, which are substantially the same as those shown in Fig. 2.

Figure 3 shows wind tunnel measurements by Blair for several carefully characterized levels of freestream turbulence with UHF. Blair's test plate had an unheated starting length, $x_0 = 4.3$ cm, so that the laminar Nusselt number follows the theoretical prediction, $Nu_{lam} \times [1 - (x_0/x)^{3/4}]^{-1/3}$ (see Appendix B), which we use as the laminar term in Eq. (9) for this case. Agreement of the laminar theory with the data is excellent. Blair's fully turbulent data converge to Eq. (6). Values of c and Re_l were fitted as before, and again the agreement with data is excellent. The value of c becomes much larger for $Re_l > 10^6$. As noted earlier, Blair concluded that freestream turbulence could increase the turbulent heat transfer coefficient, an effect that may be discernible in the data for $u_r'/u_\infty \simeq 2\%$.

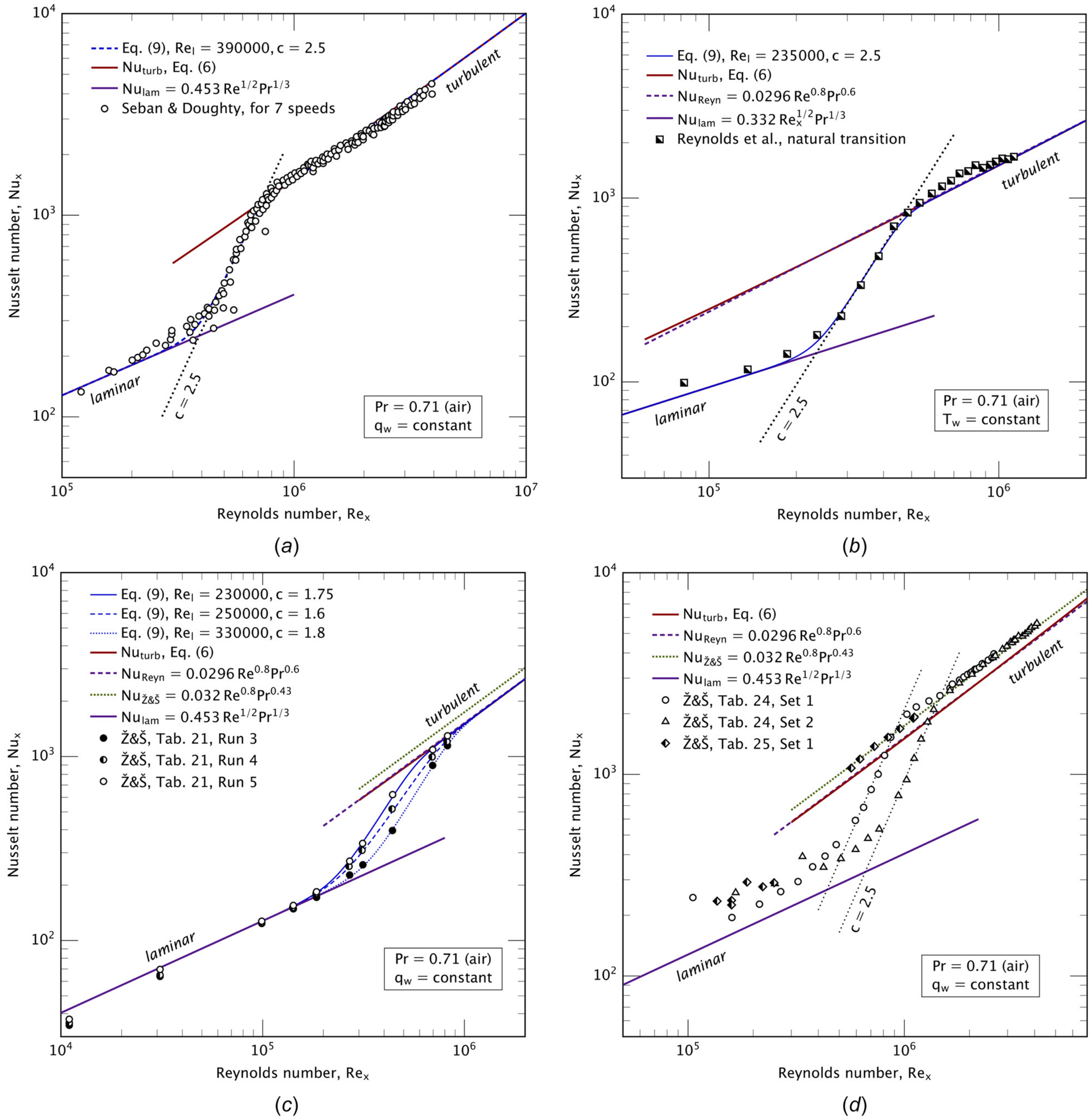

Fig. 4 Proposed correlation, Eq. (9), compared to the air data of: (*a*) Seban and Doughty (Eq. 9 mostly obscured by data) [18]; (*b*) Reynolds et al. [36]; (*c*) Žukauskas and Šlančiauskas's short plate with varied ΔT (R3, 2–7 K; R4, 7–23 K, R5, 10–34 K); and (*d*) Žukauskas and Šlančiauskas's longer plates [26]

Figure 4 shows fits through the transition region for four additional wind tunnel studies. Figure 4(*a*) shows data for seven different freestream speeds from Seban and Doughty [18]. The trend of these data for Reynolds numbers above 10^6 is 7–8% below Eq. (6). In the laminar range, the data lie above Eq. (3); however, these data were analytically corrected for an unheated starting length, a process that the authors also note contributed to greater scatter in the transition range. Beyond these two differences, the fitted values of c and Re_l put Eq. (9) into good agreement with the transition data.

Figure 4(*b*) shows the one dataset in the study of Reynolds et al. [36] for which the boundary layer had not been intentionally tripped at the leading edge. Again using the fitted parameters, Eq. (9) has good agreement with the measurements. Equation (8), proposed by Reynolds et al. for fully turbulent flow, is also shown. The data can be observed to exceed the fully turbulent line just after transition. Reynolds et al. discussed and modeled this effect, which had also been described by Seban and Doughty. They attributed the effect to differences between the momentum and energy thicknesses of an already fully turbulent boundary layer and of the boundary layer formed at the end of transition (A similar, but less pronounced effect, might be perceived in Figs. 3 and 4(*a*).).

Figure 4(*c*) shows measurements from Žukauskas and Šlančiauskas [26] for a single plate at a fixed air speed with an increasing wall heat flux. The transition Reynolds number shifts slightly lower as the plate temperature increases. Equation (9) fits each case separately.

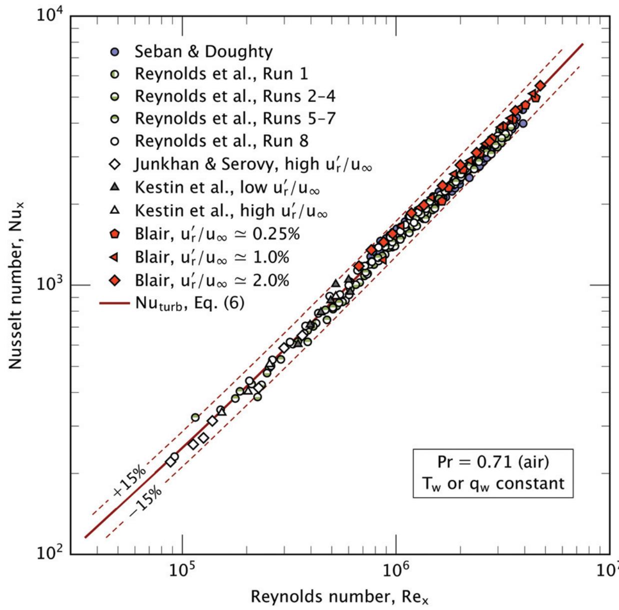

Fig. 5 Fully turbulent data from Refs. [5,10,17,18,32], including six additional data sets (Runs 2–7) from Ref. [32]. 99.4% of the data are within ±15% of Eq. (6). The sample standard deviation is 5.5%.

Figure 4(*d*) shows additional measurements from Žukauskas and Šlančiauskas from a different series of experiments. In the laminar range, the two data sets labeled Table 24[4] trend above laminar theory and have some significant scatter; the data labeled Table 25 have a large gap around the transition range are very scattered in the laminar range. The unusual laminar behavior might indicate a leading-edge influence of some unknown type (see Sec. 2.1). In the fully turbulent range, all three data sets lie in a fairly tight line about 15–25% above both Eq. (9) and measurements by other investigators; no reason for this difference is evident. However, the transition range of the Table 24 data sets is well represented by a slope $c = 2.5$, consistent with the other air data undergoing transition at similar Reynolds numbers.

Both Figs. 4(*c*) and 4(*d*) show the power-law fit proposed by Žukauskas and Šlančiauskas (for all Pr, correlating their data to roughly ±15%)

$$\mathrm{Nu}_{\mathrm{turb}} = 0.032\,\mathrm{Re}_x^{0.8}\,\mathrm{Pr}^{0.43} \tag{10}$$

together with the relationship proposed by Reynolds et al. [32]. Equation (10) is substantially higher than other correlations and data for air, presumably because is it based on the data of Fig. 4(*d*), which are also higher. Similarly, the value proposed by Žukauskas and Šlančiauskas for the term a_1 in Eq. (2) is lower than in other investigations.

Žukauskas and Šlančiauskas provide an additional dataset for high heat fluxes (not shown), with T_w/T_∞ of 1.20–1.25, for which the variable properties correction would be 7–9%. Those data do not encompass the transition range. Their trend is similar to Fig. 4(*d*), but with somewhat more scatter.

To evaluate the performance of Eq. (6), all of the fully turbulent air data from Refs. [5], [10], [17], [18], and [32] are plotted in Fig. 5. This includes the data from Figs. 2–4(*a*) as well as six additional runs from Ref. [32] that are not in Fig. 2. The standard deviation of the data around Eq. (6) is ±5.5%, for a 95% confidence interval of ±11%. Figure 5 includes 328 data points; 326 of these (99.4%) are within ±15% of Eq. (6). The air data of Ref. [26] are not included because they are systematically high relative to all other studies (relative to Eq. (6), those data are 15–25% high, with a few points 30% high). Equation (8) is very close to Eq. (6) for air.

4.2 Data for Water.

Figure 6 shows Žukauskas and Šlančiauskas' data for room temperature water. In Fig. 6(*a*), Runs 7 and 8 have the same velocity and freestream temperature, but the temperature differences in Run 8 are significantly greater (see Table 2). For Run 7, the property-ratio correction averages 2%, and for Run 8 it averages 10%. Neither correction has been applied to the correlations plotted. Both data sets show good agreement with the laminar theory, Eq. (3), and follow a transition curve with $c = 1.75$ and $\mathrm{Re}_l = 68{,}000$. (The laminar correlation would be closer to the Run 8 data if the property correction were applied.)

Figure 6(*b*) shows data extending well into the turbulent range. The proposed correlation, Eq. (9), represents the transitional and turbulent data well. Also, shown here are the correlations of Hollingsworth [27] (see Table 2) and of Žukauskas and Šlančiauskas. The turbulent data for Run 18 and Hollingsworth's correlation are close one another, although about 10% below Eq. (6). The laminar data for these experiments are quite scattered. Property ratio corrections have not been applied. For Table 27, corrections average <5%, and for the Table 25 data, corrections average <6%.

Figure 7 shows Žukauskas and Šlančiauskas' data for $\mathrm{Pr} = 2.95$, obtained using hot water in the fully turbulent regime. The expanded scale of this chart's ordinate makes the spread of data appear larger than on the other charts. Žukauskas and Šlančiauskas note that their measurement uncertainties were highest for the hot water experiments (reported as ±10%). The data lie up to 20% below Eq. (6) at the highest Reynolds numbers (around 4×10^6), and 10% below Hollingsworth's correlation. Variable properties effects on these data are negligible.

4.3 Data for Transformer Oil.

Figure 8 shows Žukauskas and Šlančiauskas' data for transformer oil at Pr of 109 and 257. For these data, property variations across the boundary layer are substantial. Therefore, the correction factor recommended by Žukauskas and Šlančiauskas, $(\mathrm{Pr}_\infty/\mathrm{Pr}_w)^{0.25}$, has been applied to the proposed correlation, Eq. (9). A single average value (the average of Žukauskas and Šlančiauskas' pointwise values) has been used. With this adjustment, agreement between the data and Eq. (9) is remarkably good.

Figure 9(*a*) shows data for $\mathrm{Pr}_\infty = 85$ compared to the proposed correlation. For these two data sets, the variable properties correction recommended by Žukauskas and Šlančiauskas averages 12.7% and 17%. The proposed correlation is plotted both without adjustment and with a +15% adjustment. The two curves bracket the data, in the turbulent regime and the later part of the transition regime; the data do not extend to laminar conditions.

Equation (6) is compared to Žukauskas and Šlančiauskas' data for fully turbulent flow of transformer oil at $\mathrm{Pr}_\infty = 55$ in Fig. 9(*b*); 13 of 16 points are within 10% of the equation (15 of 16 are within 15%). Those data do not extend to laminar and transitional conditions. The average variable properties correction for these data is <3% and is not applied to correlation.

4.4 Recommended Values of *c* and Re_l.

The value of c clearly rises as Re_l rises. Figure 10 plots c as a function of the corresponding value of Re_l for each of the data sets fitted in this paper. A few data sets have poorly defined slopes in the transition region, as a result of either limited data or high scatter (Figs. 4(*c*) and 9(*a*), and Junkhan and Serovy's low turbulence data in Fig. 2). The remaining data for $3 \times 10^4 < \mathrm{Re}_l < 5 \times 10^5$ are all within ±8% of

$$c = 0.9922\,\log_{10}\mathrm{Re}_l - 3.013 \tag{11}$$

and 80% are within ±5%. The value $c = 6$ for Blair's low turbulence data does not lie on this curve, and more data for $\mathrm{Re}_l > 5 \times 10^5$ would be needed to extend the curve fit to higher Re_l.

[4]The table numbers for Žukauskas and Šlančiauskas's data refer to the data tables in the appendix of their book [26].

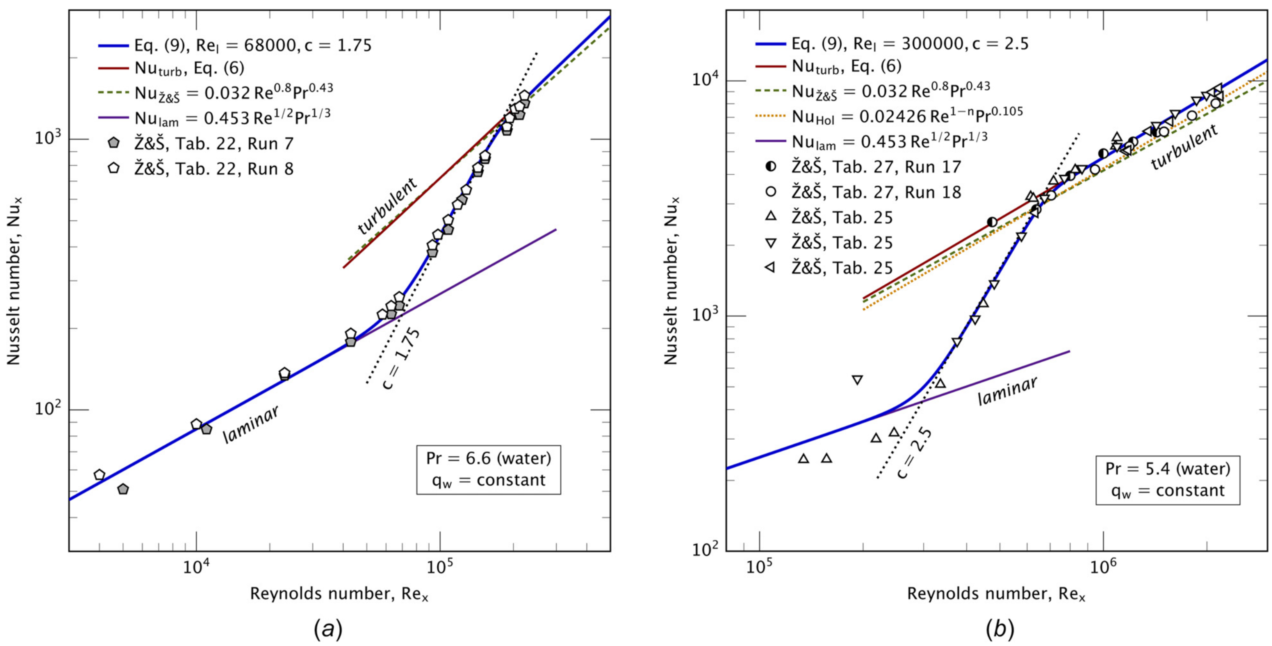

Fig. 6 Proposed correlation, Eq. (9), compared to Žukauskas and Šlančiauskas' data for water [26]: (*a*) Pr = 6.57, $u_\infty = 0.315\ \mathrm{m\,s^{-1}}$; and (*b*) Pr = 5.31–5.38, $u_\infty = 0.9$–$1.8\ \mathrm{m\,s^{-1}}$

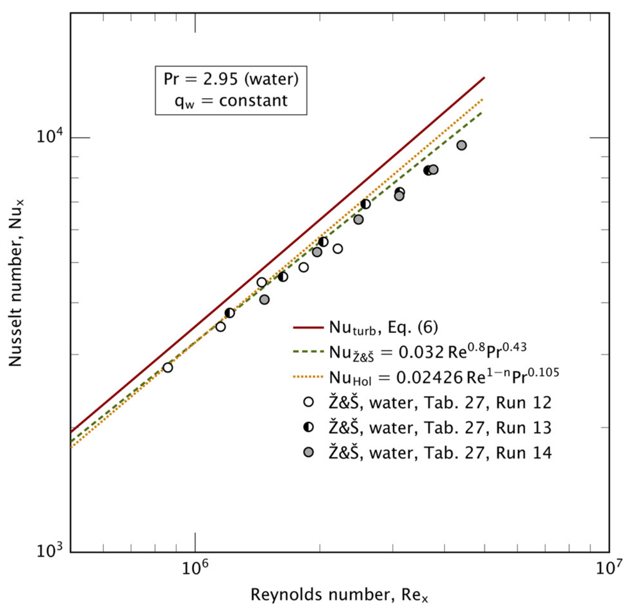

Fig. 7 More of Žukauskas and Šlančiauskas' data for hot water ($T_\infty = 60\,^\circ$C) at 1.28, 1.82, and 2.20 m s^{-1}. Variable properties correction $(\mathrm{Pr}_\infty/\mathrm{Pr}_w)^{0.25} < 2\%$. Note expanded scale relative to other figures.

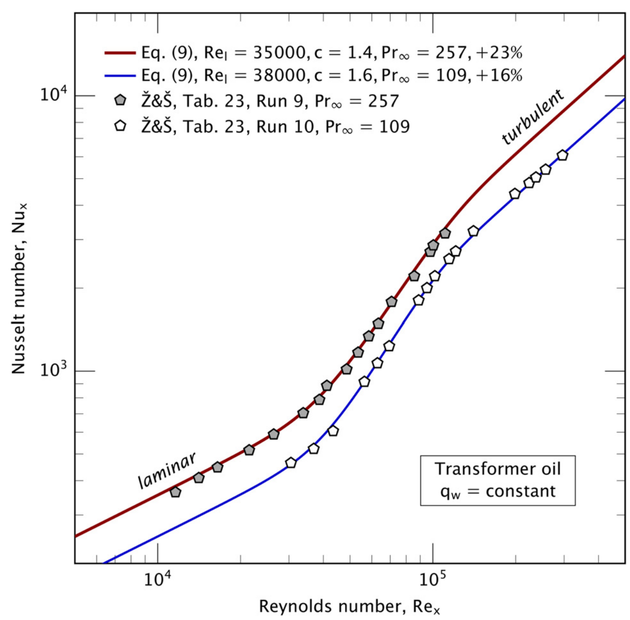

Fig. 8 Proposed correlation, Eq. (9), compared to Žukauskas and Šlančiauskas' data for transformer oil [26]. Variable properties correction $(\mathrm{Pr}_\infty/\mathrm{Pr}_w)^{0.25}$ is applied to correlation. Run 9: $T_\infty = 26.7\,^\circ$C, $\Delta T = 15$–20 K, +23% property ratio correction; Run 10: $T_\infty = 51.2\,^\circ$C, $\Delta T = 24$–31 K, +16% property ratio correction.

Figures 4(*b*) and 6(*a*) display the intersection of the laminar correlation, Eq. (3), with the dotted line representing the transition correlation, Eq. (5). The intersection lies at Re_l. The data and the fit begin to rise above the laminar value upstream of Re_l; and, at Re_l, the Nusselt number of Eq. (9) is 7% greater than the laminar Nusselt number.

Mayle [42] and Blair [34] discuss procedures for estimating the onset of transition from the local value of u'_r/u_∞. Most of the present datasets did not characterize u'_r/u_∞ locally. For the studies that did provide streamwise measurements of u'_r/u_∞ [10,17,32,34], Re_l is within about a factor of two of Mayle's empirical equation, which is equivalent to

$$\mathrm{Re}_l = (3.6 \times 10^5)(100u'_r/u_\infty)^{-5/4} \tag{12}$$

for a laminar boundary starting at the leading edge under zero pressure gradient. However, the laminar momentum boundary layers measured mostly differ from that condition and differ between the various studies. This upstream variability together with unclear local values of u'_r/u_∞ leaves Mayle's equation with little predictive power for the heat transfer experiments summarized here. When experimental conditions are better defined, Mayle's equation has good experimental support [42].

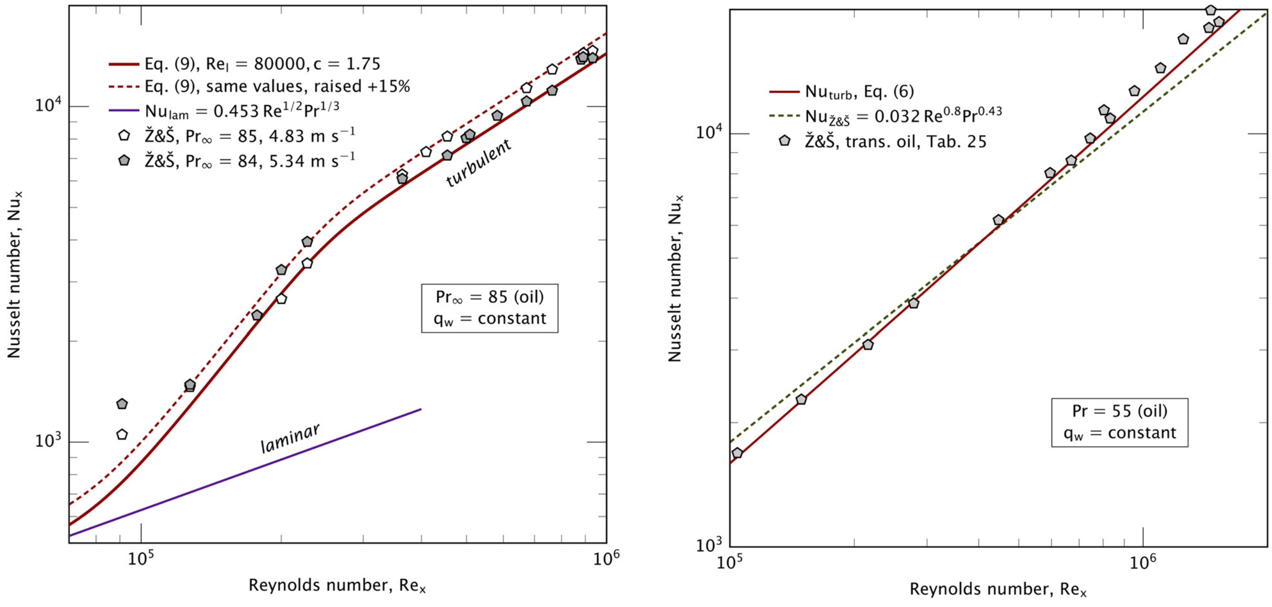

(*a*) (*b*)

Fig. 9 Žukauskas & Šlančiauskas' data for transformer oil. Average variable properties correction $(\mathrm{Pr}_\infty/\mathrm{Pr}_w)^{0.25}$: $\mathrm{Pr}_\infty = 85$, 17%; $\mathrm{Pr}_\infty = 84$, 12.7%; $\mathrm{Pr}_\infty = 55$, 2.7%. (*a*) $\mathrm{Pr}_\infty = 85$ and (*b*) $\mathrm{Pr}_\infty = 55$.

In working scenarios with significant disturbances ($u'_r/u_\infty \gtrsim 3\%$), transition is likely to begin in the range $4\times10^4 \lesssim \mathrm{Re}_l \lesssim 10^5$. Only with extremely low levels of turbulence ($u'_r/u_\infty \lesssim 0.5\%$) can Re_l exceed 10^6; Schubauer and Skramstad [16] reported an asymptotic limit of $\mathrm{Re}_l \simeq 2.8\times10^6$ for $u'_r/u_\infty < 0.1\%$.

5 Average Nusselt Number

An average Nusselt number may be found by integration, if desired. Given that Eq. (9) provides rather sharp transitions between flow regimes, piecewise integration of the component terms seems sufficient. For uniform T_w

$$\bar{h} = \frac{1}{L\Delta T}\int_0^L q_w\,dx \tag{13}$$

$$= \frac{1}{L}\left[\int_0^{x_l} h_{\text{laminar}}\,dx + \int_{x_l}^{x_u} h_{\text{trans}}\,dx + \int_{x_u}^{L} h_{\text{turbulent}}\,dx\right] \tag{14}$$

where $x_l = (\nu/u_\infty)\mathrm{Re}_l$ and $x_u = (\nu/u_\infty)\mathrm{Re}_u$. The first two integrals can be evaluated by hand. The third integral is less simple analytically, unless a power law form is adopted for the turbulent region. For instance, if we consider gas flows, Eq. (8) will suffice

$$\overline{\mathrm{Nu}}_L \equiv \frac{\bar{h}L}{k} = 0.037\,\mathrm{Pr}^{0.6}\left(\mathrm{Re}_L^{0.8} - \mathrm{Re}_u^{0.8}\right) + 0.664\,\mathrm{Re}_l^{1/2}\mathrm{Pr}^{1/3} + \underbrace{\frac{1}{c}\left(\overset{0.0296}{\cancel{0.037}}\,\mathrm{Re}_u^{0.8}\mathrm{Pr}^{0.6} - \overset{0.332}{\cancel{0.664}}\,\mathrm{Re}_l^{1/2}\mathrm{Pr}^{1/3}\right)}_{\text{contribution of transition region}} \quad \text{for gases} \tag{15}$$

As an example, we may consider a case corresponding to the low turbulence air data of Kestin et al. in Fig. 2: $\mathrm{Re}_l = 140{,}000$, $c = 2$, $\mathrm{Re}_u = 335{,}000$ with, say, $\mathrm{Re}_L = 600{,}000$. Then

$$\overline{\mathrm{Nu}}_L = \underbrace{470.7}_{\text{turb.}} + \underbrace{221.6}_{\text{lam.}} + \underbrace{\overset{259.2}{\cancel{285.4}}}_{\text{trans.}} = \overset{951.2}{\cancel{977.7}} \tag{16}$$

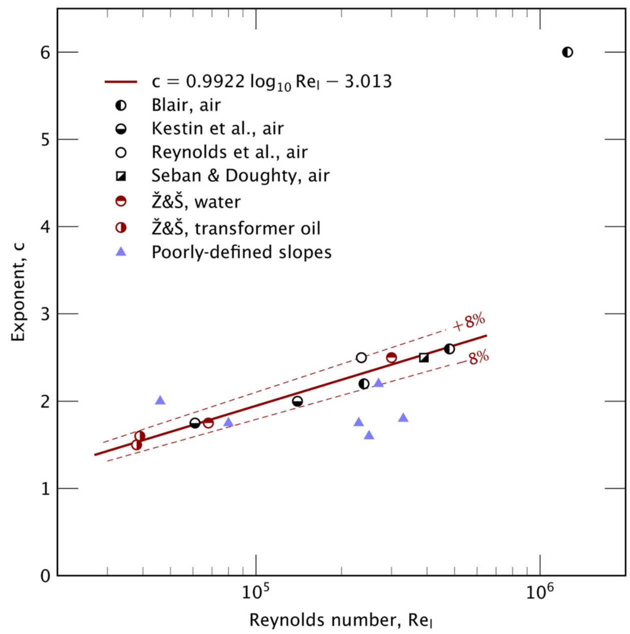

Fig. 10 The exponent *c* as a function of Re_l

The transitional region contributes 27.2% ~~29.2%~~ of the total value. If transition were omitted (abruptly changing from laminar to turbulent flow, as often illustrated in textbooks), then: (a) if transition is taken to occur at Re_l, $\overline{\mathrm{Nu}}_L = 1091$ (+11% error); but (b) if transition is taken to lie at Re_u, $\overline{\mathrm{Nu}}_L = 813.6$ (–17% error). Note also that the larger value exceeds the smaller value by 34%. The difference will be larger for smaller values of Re_L, and the difference will become smaller if Re_L increases.

6 Conclusions

New equations are proposed for calculating the Nusselt number of a flat plate boundary layer from the laminar regime, through

Table 4 Summary of the proposed correlation. Data supporting these equations span $0.7 \leqslant \mathrm{Pr} \leqslant 257$ and $4000 \leqslant \mathrm{Re}_x \leqslant 4{,}300{,}000$, with freestream turbulence levels up to 5%. Correlation applies to smooth, sharp-edged, flat plates with zero streamwise pressure gradient at either UWT or uniform heat flux (UHF).

Combining formula

$$\mathrm{Nu}_x(\mathrm{Re}_x, \mathrm{Pr}) = \left[\mathrm{Nu}_{\mathrm{lam}}^5 + (\mathrm{Nu}_{\mathrm{trans}}^{-10} + \mathrm{Nu}_{\mathrm{turb}}^{-10})^{-1/2}\right]^{1/5}$$

Laminar region

$$\mathrm{Nu}_{\mathrm{lam}}(\mathrm{Re}_x, \mathrm{Pr}) = \begin{cases} 0.332\,\mathrm{Re}_x^{1/2}\mathrm{Pr}^{1/3} & \text{UWT} \\ 0.453\,\mathrm{Re}_x^{1/2}\mathrm{Pr}^{1/3} & \text{UHF} \end{cases}$$

With an unheated starting length of x_0, use

$$\mathrm{Nu}_{\mathrm{lam}}(\mathrm{Re}_x, \mathrm{Pr}) \times [1 - (x_0/x)^{3/4}]^{-1/3}$$

Transition region

$$\mathrm{Nu}_{\mathrm{trans}}(\mathrm{Re}_x, \mathrm{Pr}) = \mathrm{Nu}_{\mathrm{lam}}(\mathrm{Re}_l, \mathrm{Pr}) \times (\mathrm{Re}_x/\mathrm{Re}_l)^c$$

Re_l is the Reynolds number at onset of transition

$$c = 0.9922\,\log_{10}\mathrm{Re}_l - 3.013 \text{ for } \mathrm{Re}_l < 5 \times 10^5$$

Turbulent region

$$\mathrm{Nu}_{\mathrm{turb}}(\mathrm{Re}_x, \mathrm{Pr}) = \frac{\mathrm{Re}_x\mathrm{Pr}\,(C_f/2)}{1 + 12.7(\mathrm{Pr}^{2/3} - 1)\sqrt{C_f/2}}$$

$$C_f(\mathrm{Re}_x) = \frac{0.455}{[\ln(0.06\,\mathrm{Re}_x)]^2}$$

For gases only, the following equation has similar accuracy

$$\mathrm{Nu}_{\mathrm{turb}}(\mathrm{Re}_x, \mathrm{Pr}) = 0.0296\,\mathrm{Re}_x^{0.8}\,\mathrm{Pr}^{0.6} \quad \text{for gases}$$

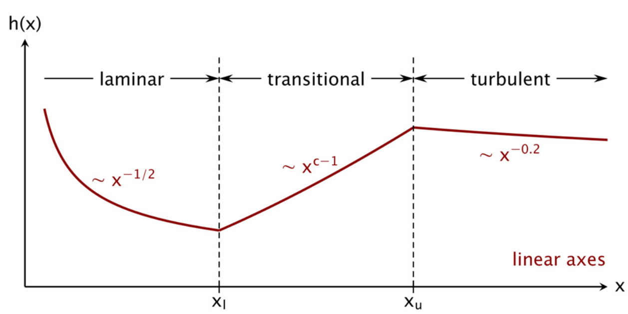

Fig. 11 Variation of the heat transfer coefficient, $h(x)$, in a flat-plate boundary layer. The transition region has a length similar to the laminar region and must be taken into account.

the transition region, and into the fully turbulent region. These formulas are in good agreement with available data for air, water, and oil boundary layers spanning the ranges $0.7 \leqslant \mathrm{Pr} \leqslant 257$, $4000 \leqslant \mathrm{Re}_x \leqslant 4{,}300{,}000$, with freestream turbulence levels up to 5%. The complete correlation is summarized in Table 4.

(1) The transition region has a length similar to the laminar region, as shown in Fig. 11.
(2) Data show that the Nusselt number in the transition region varies as Re_x^c where the exponent c increases with an increase in Re_l, the Reynolds number at the onset of transition. Through the examination of many independent experiments, values of c are fitted as a function of Re_l. The transition regime is described by Eqs. (5) and (11).
(3) Churchill's multiregion correlation is modified to accurately predict the local Nusselt number in the transition and turbulent ranges. The new correlation, Eq. (9), shows good agreement with a large number of experimental data drawn from many independent studies.
(4) Equation (6) correlates the fully turbulent air data to $\pm 11\%$ (two standard deviations); 99.4% of the data are within $\pm 15\%$.
(5) The fully turbulent air data of Žukauskas and Šlančiauskas are systematically higher than air data from other investigators. Similarly, their correlation, Eq. (10), is higher for air than other correlations.
(6) The data of Fage and Falkner, for UHF laminar air flow, are in good agreement with corresponding analytical results, contrary to the suggestion of Jakob and Dow, down to an overall Reynolds number of 1400 (Appendix B).
(7) Very few measurements are available for heat transfer in turbulent liquid boundary layers.
(8) Older literature on convection contains a great deal of information that remains useful today.

Acknowledgment

I am grateful for useful suggestions from Leon R. Glicksman (MIT), Je-Chin Han (Texas A&M University), D. Keith Hollingsworth (University of Alabama, Huntsville), and John H. Lienhard, IV (University of Houston).

Nomenclature

Roman Letters

a = coefficient in Eq. (3)
b = coefficient in Eq. (4)
c = exponent on Reynolds number, Eq. (4)
C_f = local skin friction coefficient
d = coefficient in Churchill's function ϕ
f = Darcy friction factor
h = local heat transfer coefficient, W m^{-2} K^{-1}
$\bar{h}$ = average heat transfer coefficient, W m^{-2} K^{-1}
$I(u_0)$ = integral defined by Eq. (B7)
k = thermal conductivity of fluid, W m^{-1} K^{-1}
Nu_x = local Nusselt number, hx/k
$\overline{\mathrm{Nu}}_L$ = average Nusselt number, $\bar{h}L/k$
p = exponent in Eq. (1)
Pr = Prandtl number
q_w = wall heat flux, W m^{-2}
q_0 = a uniform heat flux, W m^{-2}
Re_x = local Reynolds number, $u_\infty x/\nu$
Re_L = overall Reynolds number, $u_\infty L/\nu$
s = exponent in Eq. (1)
St = local Stanton number, $\mathrm{Nu}_x/\mathrm{Re}_x\,\mathrm{Pr}$
T_w = wall temperature, K
T_∞ = freestream temperature, K
$u_0 = 1 - (x_0/x)^{3/4}$
u_∞ = mean freestream speed, m s^{-1}
u_r' = r.m.s. fluctuation of freestream speed, m s^{-1}
x = distance from leading edge, m
x_0 = unheated starting length, m

Greek Symbols

$\mathrm{B}(n, m)$ = beta function
$\Gamma(x)$ = gamma function
$\Delta T = T_w - T_\infty$, K
ν = kinematic viscosity of fluid, m^2 s^{-1}
σ = standard deviation
ϕ = Churchill's function, Eq. (A2)

Subscripts

av = average over surface
l = at lower Re of transition region

lam = local value in the laminar region
trans = local value in the transition region
turb = local value in the turbulent region
u = at upper Re of transition region
w = value at the wall
∞ = value in freestream

Abbreviations

r.m.s. = root-mean-square
UHF = uniform heat flux
UWT = uniform wall temperature

Appendix A: Churchill's Correlation in Full

Churchill's correlation [2] is

$$\mathrm{Nu}_x = 0.45 + \left(0.3387\,\phi^{1/2}\right)\left\{1 + \frac{(\phi/2,600)^{3/5}}{\left[1+(\phi_u/\phi)^{7/2}\right]^{2/5}}\right\}^{1/2} \tag{A1}$$

where

$$\phi \equiv \mathrm{Re}_x \mathrm{Pr}^{2/3}\left[1+\left(\frac{0.0468}{\mathrm{Pr}}\right)^{2/3}\right]^{-1/2} \tag{A2}$$

and ϕ_u is a number typically between about 10^5 and 10^7. The actual value of ϕ_u must be fit to each specific dataset. If the Reynolds number at the end of the transition region is Re_u, an estimate is $\phi_u \approx \phi(\mathrm{Re}_x = \mathrm{Re}_u)$.

The equation is for uniform T_w. To adapt it to uniform q_w, the constants 0.3387, 0.0468, and 2600 are replaced by 0.4637, 0.02052, and 7420, respectively.[5] Churchill gave a similar equation for the average Nusselt number.

This equation embeds a transition slope of $c = 1.5$. At high Reynolds number (fully turbulent flow), the equation limits to

$$\mathrm{Nu}_x \xrightarrow{\mathrm{Re}_x \gg \mathrm{Re}_u} 0.032\phi^{4/5} \xrightarrow{\mathrm{Pr}\gg 1} 0.032\,\mathrm{Re}_x^{0.8}\,\mathrm{Pr}^{8/15} \tag{A3}$$

Appendix B: Laminar Boundary Layer With Uniform Heat Flux

The laminar similarity solution for uniform heat flux is not well known: even recently, some well-respected books report that there is no such solution [19]. This appendix provides that background, as well as sketching the UHF solution with an unheated starting length, which is less well known than that for UWT.

B.1 Uniform Flux Over Entire Plate. The similarity transformation for $\Delta T \sim x^n$ was first discussed in 1931 by Fage and Falkner [7], who gave a perturbation solution, but the ordinary differential equation was not integrated until 1949 by Chapman and Rubesin [43]. The first numerical integrations for $n = 1/2$, corresponding to uniform wall heat flux, were due to Sugawara and Sato [44] in 1951 and Levy [45] in 1952. A linear regression on Levy's four computed points for $n = 1/2$ (Pr of 0.7, 2, 10, 20) leads to

$$\mathrm{Nu}_x = 0.4542\,\mathrm{Re}_x^{1/2}\,\mathrm{Pr}^{0.3301} \tag{B1}$$

Various analytical results from this era are summarized by Imai [46]. Imai obtained an asymptotic solution for high Pr using the WKB method

$$\frac{\mathrm{Nu}_x}{\mathrm{Re}_x^{1/2}} = \frac{\Gamma(2/3)\,A^{1/3}}{2^{1/2}\,3^{2/3}\,\Gamma(4/3)} \quad \text{with} \quad A = (1/2+2n)\sqrt{2}(0.33206)\mathrm{Pr} \tag{B2}$$

For $n = 1/2$

$$\mathrm{Nu}_x = 0.4587\,\mathrm{Re}_x^{1/2}\,\mathrm{Pr}^{1/3} \tag{B3}$$

Imai reported 1% agreement with Levy's numerical values down to Pr = 0.7, which is within the accuracy of Levy's numerics.

Further, Fage and Falkner's experimental values for air fit well to $\overline{\mathrm{Nu}}_L = 0.75\,\mathrm{Re}_L^{1/2}$, based on a value of k_{mean} that is 12% lower than modern property data. The temperature ratio, $T_{w,\mathrm{av}}/T_\infty = 1.45$, is high enough that variable properties effects are not negligible. Without a variable properties correction, the experiments are within +9% of Imai's formula. If a correction of $(T_{w,\mathrm{av}}/T_\infty)^{-0.4}$ is applied, the agreement is –6%.

B.2 Uniform Flux With Unheated Starting Length. Tribus and Klein [47,48] gave general equations for variable flux, working from the cubic integral-method solution for an unheated starting length

$$T_w - T_\infty = A(x)\int_0^x \left[1-\left(\frac{\xi}{x}\right)^{3/4}\right] q_w(\xi)\,d\xi \tag{B4}$$

Here, $A(x) = C/k\,\mathrm{Re}_x^{1/2}\,\mathrm{Pr}_x^{1/3}$, where $1/C = 6\Gamma(4/3)\Gamma(5/3)c_1$ with $c_1 = (3/2)(1/20)^{1/3}(13/280)^{1/6} = 0.331293$ (from the integral solutions) so that $C = 0.624065$. For an unheated starting length

$$q_w(x) = \begin{cases} 0 & \text{for } x < x_0 \\ q_0 & \text{for } x \geqslant x_0 \end{cases} \tag{B5}$$

and

$$\frac{T_w - T_\infty}{A(x)q_0} = \int_{x_0}^x \left[1-\left(\frac{\xi}{x}\right)^{3/4}\right] d\xi \tag{B6}$$

Setting $u = 1-(\xi/x)^{3/4}$, $u_0 = 1-(x_0/x)^{3/4}$, and $s = u/u_0$, some algebra leads to

$$\frac{3(T_w - T_\infty)}{4xA(x)q_0u_0^{1/3}} = I(u_0) \equiv \int_0^1 s^{-2/3}(1-u_0 s)^{1/3}\,ds \tag{B7}$$

Hence

$$\mathrm{Nu}_x \equiv \frac{q_0 x}{(T_w - T_\infty)k} = \frac{3}{4kA(x)u_0^{1/3}I(u_0)} = \frac{3\,\mathrm{Re}_x^{1/2}\,\mathrm{Pr}_x^{1/3}}{4Cu_0^{1/3}I(u_0)} \tag{B8}$$

We can easily bound the integral $I(u_0)$. Setting $u_0 = 0$

$$I(u_0) \leqslant I(0) = \int_0^1 s^{-2/3}\,ds = 3 \tag{B9}$$

Setting $u_0 = 1$ and identifying the beta and gamma functions

$$I(u_0) \geqslant I(1) = \int_0^1 s^{-2/3}(1-s)^{1/3}\,ds = \mathrm{B}(1/3, 4/3) \tag{B10}$$

$$= \frac{\Gamma(1/3)\Gamma(4/3)}{\Gamma(5/3)} = 2.649958\cdots \tag{B11}$$

These bounds are tight ($2.649958/3 = 0.883$). If we make the approximation $I(u_0) \simeq I(1)$, then,

[5]Churchill seems to have overlooked the need for the last substitution. Equation (A1) corrects a typographical error in Churchill's Eq. (16).

$$\mathrm{Nu}_x \simeq \frac{3\,\mathrm{Re}_x^{1/2}\,\mathrm{Pr}_x^{1/3}}{4Cu_0^{1/3}I(1)} \tag{B12}$$

$$= \frac{\mathrm{Re}_x^{1/2}\,\mathrm{Pr}_x^{1/3}}{[1-(x_0/x)^{3/4}]^{1/3}}\frac{3}{4(0.624065)(2.649958)} \tag{B13}$$

$$= 0.4535\,\frac{\mathrm{Re}_x^{1/2}\,\mathrm{Pr}_x^{1/3}}{[1-(x_0/x)^{3/4}]^{1/3}} \tag{B14}$$

What is key here is that the approximation is bounded within 12% right up to x_0.

The case $u_0 = 1$ corresponds to $x_0 = 0$, a uniform wall heat flux over the entire length, as commonly given in textbooks [6,19]

$$\mathrm{Nu}_x = 0.4535\,\mathrm{Re}_x^{1/2}\,\mathrm{Pr}_x^{1/3} \tag{B15}$$

This result is within 1% of Imai's formula.

Appendix C: Comments on the Classical Colburn Analogy

The classical Reynolds–Colburn (or Chilton–Colburn) analogy, from 1933 (and 1934), has the form [22,23]

$$\mathrm{St} = \frac{C_f}{2}\,\mathrm{Pr}^{-2/3} \tag{C1}$$

By combining this expression with an equation for C_f as power of the Reynolds number, the Nusselt number can be expressed as a product of powers of the Reynolds and Prandtl numbers. Such equations have commonly been used for turbulent boundary layers and turbulent pipe flows.

Unfortunately, these power laws cannot accurately span a wide range of Prandtl number: at high Reynolds numbers, the dependence of the Reynolds number exponent on the Prandtl number becomes significant so that a single, fixed exponent for Re and for Pr is inadequate to cover a wide range of conditions. Gnielinski [30] and Žukauskas and Šlančiauskas [26] discuss this point with reference to experimental data for either pipe or boundary layer flows. Transport models that take account of the structure of the turbulent boundary layer result in expressions having the general form of Eq. (2) [24,26,28,29]. Those expressions are capable of covering the full range of Prandtl number [29,30]. For a narrow range of Pr (say, just for gases or for some range of liquids), power-law formulas can be quite accurate, as shown by Gnielinski.

Colburn considered a wide spectrum of data in his work, but neither Colburn [22] nor Chilton and Colburn [23] had much data for external boundary layers. And the data they had were only for gases. Chilton and Colburn included three data points for evaporation of water into laminar air flow. In the turbulent regime, Colburn referred to two somewhat scattered sets of air data. In the laminar rage, Colburn used the UHF air data of Fage and Falkner [7], showing good agreement with Eq. (35); but he later confessed to Jakob and Dow that he had made a "slide-rule error" in plotting these data [9] and that the points should have been 21% higher. In fact, the Colburn analogy is incapable of discriminating the laminar thermal boundary condition.

Appendix D: Typical Values of Prandtl Number

Values of the Prandtl number for the fluids discussed in this paper are given in Table 5.

Table 5 Values of Pr for the fluids discussed in this paper

Fluid	T (°C)	Pr	Fluid	T (°C)	Pr
Liquid metals	Typical	≲0.05	Air	−100 to 1200	0.70 to 0.74
Water	22	6.66	Transformer oil	30	222
	27	5.85		40	153
	32	5.18		50	112.6
	37	4.63		60	85.6
	47	3.77		70	68.2
	67	2.68		80	55.2
	87	2.03		90	46.8

Transformer oil data are from Ref. [26]; other values are from Ref. [6].

References

[1] Whitaker, S., 1972, "Forced Convection Heat Transfer Correlation for Flow in Pipes Past Flat Plates, Single Cylinders, Single Spheres, and for Flow in Packed Beds and Tube Bundles," AIChE J., **18**(2), pp. 361–371.

[2] Churchill, S. W., 1976, "A Comprehensive Correlating Equation for Forced Convection From Flat Plates," AIChE J., **22**(2), pp. 264–268.

[3] Churchill, S. W., and Usagi, R., 1974, "A Standardized Procedure for the Production of Correlations in the Form of a Common Empirical Equation," Ind. Eng. Chem. Fund., **13**(1), pp. 39–44.

[4] Churchill, S. W., and Ozoe, H., 1973, "Correlations for Laminar Forced Convection in Flow Over an Isothermal Flat Plate and in Developing and Fully Developed Flow in an Isothermal Tube," ASME J. Heat Transfer, **95**(1), pp. 78–84.

[5] Blair, M. F., 1983, "Influence of Free-Stream Turbulence on Turbulent Boundary Layer Heat Transfer and Mean Profile Development: Part I—Experimental Data," ASME J. Heat Transfer, **105**(1), pp. 33–40.

[6] Lienhard, J. H., IV, and Lienhard, J. H., V, 2019, *A Heat Transfer Textbook*, 5th ed., Dover Publications, Mineola, NY.

[7] Fage, A., and Falkner, V. M., 1931, "Relation Between Heat Transfer and Surface Friction for Laminar Flow," Aeronautical Research Committee, London, Reports and Memoranda No. 1408.

[8] Pohlhausen, E., 1921, "Der Wärmeaustausch zwischen festen Körpern und Flüssigkeiten mit kleiner reibung und kleiner Wärmeleitung," ZAMM—Z. für Angew. Mathematik und Mech., **1**(2), pp. 115–121.

[9] Jakob, M., and Dow, W. M., 1946, "Heat Transfer From a Cylindrical Surface to Air in Parallel With and Without Unheated Starting Sections," Trans. ASME, **68**(2), pp. 123–134.

[10] Kestin, J., Maeder, P. F., and Wang, H. E., 1961, "The Influence of Turbulence on the Transfer of Heat From Plates With and Without a Pressure Gradient," Int. J. Heat Mass Transfer, **3**(2), pp. 133–154.

[11] Sugawara, S., Sato, T., Komatsu, H., and Osaka, H., 1958, "The Effect of Free-Stream Turbulence on Heat Transfer From a Flat Plate," NASA, Washington, DC, Memorandum No. 1441.

[12] Sugawara, S., Sato, T., and Yoshimura, S., 1951, "Experimental Researches on Heat Transfer on the Surface of Flat Plate in Forced Flow (1st Report)," Trans. Jpn. Soc. Mech. Eng., **17**(62), pp. 122–129.

[13] Dryden, H. L., Schubauer, G. B., Mock, W. C., Jr., and Skramstad, H. K., 1937, "Measurements of Intensity and Scale of Wind-Tunnel Turbulence and Their Relation to the Critical Reynolds Number of Spheres," NACA, Washington, DC, Report No. NACA-TR-581.

[14] Batchelor, G. K., 1953, *The Theory of Homogeneous Turbulence*, Cambridge University Press, Cambridge, UK.

[15] Edwards, A., and Furber, B. N., 1956, "The Influence of Free-Stream Turbulence on Heat Transfer by Convection From an Isolated Region of a Plane Surface in Parallel Air Flow," Proc. Inst. Mech. Eng. London, **170**(1), pp. 941–954.

[16] Schubauer, G. B., and Skramstad, H. K., 1948, "Laminar-Boundary-Layer Oscillations and Transition on a Flat Plate," NACA, Washington, DC, Report No. 909.

[17] Junkhan, G. H., and Serovy, G. K., 1967, "Effects of Free-Stream Turbulence and Pressure Gradient on Flat-Plate Boundary-Layer Velocity Profiles and on Heat Transfer," ASME J. Heat Transfer, **89**(2), pp. 169–175.

[18] Seban, R. A., and Doughty, D. L., 1956, "Heat Transfer to Turbulent Boundary Layers With Variable Free-Stream Velocity," Trans. ASME, **78**(1), pp. 217–223.

[19] Kays, W. M., Crawford, M. E., and Weigand, B., 2005, *Convective Heat and Mass Transfer*, 4th ed., McGraw-Hill Book Company, New York.

[20] Clauser, F. H., 1956, "The Turbulent Boundary Layer," *Advances in Applied Mechanics*, H. Dryden and T. von Kármán, eds., Vol. 4, Elsevier, Amsterdam, The Netherlands, pp. 1–51.

[21] Pope, S. B., 2000, *Turbulent Flows*, Cambridge University Press, Cambridge, UK.

[22] Colburn, A. P., 1933, "A Method of Correlating Forced Convection Heat Transfer Data and a Comparison With Fluid Friction," Trans. Amer. Inst. Chem. Eng., **29**, pp. 174–206.

[23] Chilton, T. H., and Colburn, A. P., 1934, "Mass Transfer (Absorption) Coefficients Prediction From Data on Heat Transfer and Fluid Friction," Ind. Eng. Chem., **26**(11), pp. 1183–1187.

[24] von Kármán, T., 1939, "The Analogy Between Fluid Friction and Heat Transfer," Trans. ASME, **61**(11), pp. 705–710.
[25] White, F. M., 1974, *Viscous Fluid Flow*, McGraw-Hill Book Company, New York.
[26] Žukauskas, A., and Šlančiauskas, A., 1987, *Heat Transfer in Turbulent Fluid Flows*, Hemisphere Publishing Corp, Washington, DC.
[27] Hollingsworth, D. K., Jr, 1989, "Measurement and Prediction of Turbulent Thermal Boundary Layer in Water on Flat and Concave Surfaces," Ph.D. thesis, Stanford University, Stanford, CA.
[28] Prandtl, L., 1928, "Bemerkung über den Wärmeübergang im Rohr," Phys. Z., **29**, pp. 487–489.
[29] Petukhov, B. S., 1970, "Heat Transfer and Friction in Turbulent Pipe Flow With Variable Physical Properties," *Advances in Heat Transfer*, T. F. Irvine, Jr. and J. P. Hartnett, eds., Vol. 6, Academic Press, New York, pp. 504–564.
[30] Gnielinski, V., 1976, "New Equations for Heat and Mass Transfer in Turbulent Pipe and Channel Flow," Int. Chem. Eng., **16**(2), pp. 359–368 (Also in German as Gnielinski, V., 1975, Forsch Ing-Wes, **41**(1), pp. 8–16).
[31] Hollingsworth, D. K., Kays, W. M., and Moffat, R. J., 1989, "The Measurement and Prediction of Heat Transfer in a Turbulent Boundary Layer in Water," Proceedings Seventh Symposium on Turbulent Shear Flows, Stanford, CA, Aug. 21–23, pp. 20.4.1–20.4.6.
[32] Reynolds, W. C., Kays, W. M., and Kline, S. J., 1958, "Heat Transfer in the Incompressible Turbulent Boundary Layer: I—Constant Wall Temperature," NASA, Washington, DC, Memorandum 12-1-58W.
[33] Blair, M. F., 1983, "Influence of Free-Stream Turbulence on Turbulent Boundary Layer Heat Transfer and Mean Profile Development: Part II—Analysis of Results," ASME J. Heat Transfer, **105**(1), pp. 41–47.
[34] Blair, M. F., 1982, "Influence of Free-Stream Turbulence on Boundary Layer Transition in Favorable Pressure Gradients," J. Eng. Power, **104**(4), pp. 743–750.
[35] Junkhan, G. H., 1964, "The Effects of Free-Stream Turbulence on Heat Transfer From a Flat Plate With a Pressure Gradient," Ph.D. thesis, Iowa State University of Science and Technology, Ames, IA.
[36] Reynolds, W. C., Kays, W. M., and Kline, S. J., 1958, "Heat Transfer in the Incompressible Turbulent Boundary Layer. IV–Effect of Location of Transition and Prediction of Heat Transfer in a Known Transition Region," NASA, Washington, DC, Memorandum 12-4-58W.
[37] Johnson, P. L., 1989, "The Effects of Grid-Generated Turbulence on Flat and Concave Turbulent Boundary Layers," Ph.D. thesis, Stanford University, Stanford, CA.
[38] Parmelee, G. V., and Huebscher, R. G., 1947, "Heat Transfer by Forced Convection Along a Smooth Flat Surface," Heat., Pip., Air Cond., **19**(8), pp. 115–118.
[39] Zhukauskas, A. A., and Ambrazyavichyus, A. B., 1961, "Heat Transfer From a Plate in a Liquid Flow," Int. J. Heat Mass Transfer, **3**(4), pp. 305–309.
[40] Dennis, S. C. R., and Smith, N., 1966, "Forced Convection From a Heated Flat Plate," J. Fluid Mech., **24**(3), pp. 509–519.
[41] White, F. M., 1969, "A New Integral Method for Analyzing the Turbulent Boundary Layer With Arbitrary Pressure Gradient," J. Basic Eng., **91**(3), pp. 371–378.
[42] Mayle, R. E., 1991, "The Role of Laminar-Turbulent Transition in Gas Turbine Engines," International Gas Turbine and Aeroengine Congress and Exposition, American Society of Mechanical Engineers, Orlando, FL, Jun. 3–6, Paper No. 91-GT-261.
[43] Chapman, D. R., and Rubesin, M. W., 1949, "Temperature and Velocity Profiles in the Compressible Laminar Boundary Layer With Arbitrary Distribution of Surface Temperature," J. Aeronaut. Sci., **16**(9), pp. 547–565.
[44] Sugawara, S., and Sato, T., 1951, "Heat Transfer at Laminar Boundary Layer of Flat Plate With Temperature Gradient on Its Surface," Trans. Jpn. Soc. Mech. Eng., **17**(62), pp. 137–142.
[45] Levy, S., 1952, "Heat Transfer to Constant-Property Laminar Boundary-Layer Flows With Power-Function Free-Stream Velocity and Wall-Temperature Variation," J. Aeronaut. Sci., **19**(5), pp. 341–348.
[46] Imai, I., 1958, "On the Heat Transfer to Constant-Property Laminar Boundary Layer With Power-Function Free-Stream Velocity and Wall-Temperature Distributions," Quart. Appl. Math., **16**(1), pp. 33–45.
[47] Klein, J., and Tribus, M., 1953, "Forced Convection From Nonisothermal Surfaces," Heat Transfer, A Symposium Held at the University of Michigan During the Summer of 1952, Engineering Research Institute, University of Michigan, Ann Arbor, MI, pp. 211–235.
[48] Tribus, M., and Klein, J., 1955, "Forced Convection Through a Laminar Boundary Layer Over an Arbitrary Surface With an Arbitrary Temperature Variation," J. Aeronaut. Sci., **22**(1), pp. 62–64.